Scientific
Research
Publishing

Characteristics of La$_{0.7}$Sr$_{0.3}$MnO$_3$ Films Modified by Aluminum Ions Implantation and Post-Implantation Annealing

Shaoqun Jiang[1*], Gang Wang[1], Xinxin Ma[2], Guangze Tang[2]

[1]College of Mechanics and Materials, Hohai University, Nanjing, China
[2]School of Materials Science and Engineering, Harbin Institute of Technology, Harbin, China
Email: [*]sqjhit@126.com

Abstract

The magnetron sputtered La$_{0.7}$Sr$_{0.3}$MnO$_3$ films were implanted with different doses (5×10^{15} ions·cm^{-2} and 5×10^{16} ions·cm^{-2}) of Al ions at different negative pulsed voltages (30 kV and 50 kV) by plasma based ion implantation and then annealed at 973 K for 1 h in air. The microstructure, surface morphologies, surface roughness, metal-insulator transition and room temperature emittance properties of the post-implantation annealed films were investigated and compared with those of the La$_{0.7}$Sr$_{0.3}$MnO$_3$ film annealed at 973 K for 1 h in air. The results indicate that the post-implantation annealed films show single perovskite phase and obvious (100) preferred orientation growth. The Mn-O bond length, surface roughness and metal-insulator transition temperature (T_{MI}) of the films can be effectively adjusted by changing implantation voltage or implantation dose of Al ions. However, the change of implantation parameters just has a small effect on room temperature emittance of the films. Compared with the annealed film, the post-implantation annealed films have shorter Mn-O bond length and lower room temperature emittance. The T_{MI} of the films implanted at low voltage is lower than that of the annealed film, which mainly results from the degradation of oxidization during annealing process and the part displacement of Mn^{3+}-O^{2-}-Mn^{4+} double exchange channels by Al^{3+}-O^{2-}-Mn^{4+}. The post-implanted annealed film implanted at 50 kV/5×10^{16} ions·cm^{-2} has a higher T_{MI} than the annealed film, which is 247 K. The increase of T_{MI} of the film implanted with high dose of Al ions at high voltage can be attributed to the improvement of microstructure.

1. Introduction

ABO$_3$ type perovskite manganites La$_{1-x}$M$_x$MnO$_3$ (M = Ca, Sr or Ba) with appropriate doping concentration (x)

[*]Corresponding author.

have a variable emittance property based on the metal-insulator transition [1]-[3]. With the increase of temperature, they change from low emissive metal state to high emissive insulator state. Moreover, the emissivity exhibits drastic change in the vicinity of the metal-insulator transition temperature (T_{MI}) [4] [5]. Due to the unique regulation capability of heat dissipation, these compounds have potential application for a smart cool radiator, which can automatically self-adjust its emissivity in response to the variations of environmental temperature and thermal load [6] [7]. In order to get good thermal control effect, the emittance property of $La_{1-x}M_xMnO_3$ should be adjusted to meet different thermal control applications because of the difference of thermal control demands. Generally, the emissivity of $La_{1-x}M_xMnO_3$ is mainly affected by the composition, structure, metal-insulator transition temperature and surface state, etc. The T_{MI} is especially important, which determines the thermal control temperature range of $La_{1-x}M_xMnO_3$ [8]. The relative researches indicated that the changes of doping metal element and doping concentration could result in different structure and T_{MI} of $La_{1-x}M_xMnO_3$ [9]-[11]. Therefore, the researchers adjusted the composition, microstructure and T_{MI} of $La_{1-x}M_xMnO_3$ mainly by changing doping element and doping concentration at A-site, so as to gain a series of $La_{1-x}M_xMnO_3$ with different emittance property [3] [12] [13]. From a technical feasibility viewpoint, the emissivity of $La_{1-x}M_xMnO_3$ can also be adjusted by modification methods. Ion implantation is an effective surface modification technology which can lead to a controlled introduction of defects and dopants in a material system and generate different surface properties [14] [15]. So it is worthwhile to try to adjust the emissivity of $La_{1-x}M_xMnO_3$ by ion implantation.

The modification effect of ion implantation strongly depends on the kind of implanted ions. Aluminum has a low density and is easy to be oxidized. Thus implanting with aluminum cannot obviously increase the volume density but potentially improves oxygen content of $La_{1-x}M_xMnO_3$. Meanwhile, this treatment also affects the double exchange interaction. It means that the structure, composition and T_{MI} of $La_{1-x}M_xMnO_3$ will change, which will result in different emittance properties. Up to now, the investigation on microstructure and properties especially the emittance property of $La_{1-x}M_xMnO_3$ implanted with aluminum is very little. Therefore, In this work, the $La_{0.7}Sr_{0.3}MnO_3$ films were implanted with aluminum at various negative pulsed voltages and implantation doses by plasma based ion implantation and post-implantation annealed in air. The structure, surface state, metal-insulator transition and room temperature emittance property of the modified films have been studied.

2. Experimental

The $La_{0.7}Sr_{0.3}MnO_3$ films were deposited on Si(100) by DC magnetron sputtering from a $La_{0.7}Sr_{0.3}MnO_3$ ceramic target. During deposition process, the Si substrate was kept at 853 K. The deposition was carried out in Ar (75 vol %) + O_2 (25 vol %) ambience at a total pressure of 0.5 Pa. The thickness of the films was about 700 - 750 nm. After deposition, the films were implanted with aluminum at negative pulsed voltages and then were annealed in air. The treatment parameters are shown in **Table 1**. In order to clarify implantation effect, the corresponding results of the $La_{0.7}Sr_{0.3}MnO_3$ annealed at 973 K for 1h in air were also given.

The phase structure of the films was confirmed by Glance angle X-ray diffraction (GXRD) using Cu Kα radiation and 5° angle. The surface morphologies and mean roughness of the films were studied by atomic force microscope (AFM). The bond structure and IR reflectance spectra at room temperature of the films were examined using Fourier transform infrared spectroscopy (FTIR). The resistivity was measured as a function of the temperature using the standard four-probe method between 10K and 325 K in zero field.

3. Results and Discussion

3.1. Structure of the Films

Figure 1 gives the GXRD patterns of the annealed and post-implantation annealed $La_{0.7}Sr_{0.3}MnO_3$ films. All of the films exhibit single perovskite phase. No aluminum or aluminum compound phase can be detected in the

Table 1. Parameters of implanting with aluminum and post-implantation annealing of $La_{0.7}Sr_{0.3}MnO_3$ films.

Film	Implantation voltage (V)	Implantation dose (ions·cm^{-2})	Annealing treatment
1	-	-	
2	30	5×10^{15}	
3	50	5×10^{15}	Annealing at 973 K for 1 h in air
4	50	5×10^{16}	

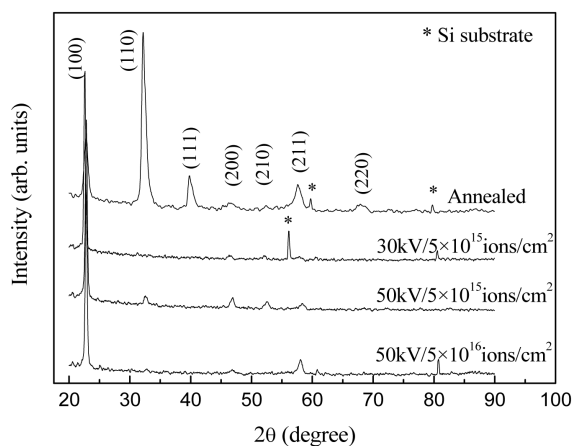**Figure 1.** GXRD patterns of the annealed and post-implantation annealed $La_{0.7}Sr_{0.3}MnO_3$ films.

post-implantation annealed films due to low Al concentration. However, the treatment of implanting with Al and post-implantation annealing makes the phase structure of the films quite different from that of the annealed film. The annealed film has a phase structure similar to that of the corresponding bulk with same composition. The post-implantation annealed films show quite obvious (100) preferred orientation growth and the degree of preferred orientation depends on the implantation voltage and implantation dose. By comparison, the post-implantation annealed film implanted at 30 kV/5×10^{15} ions·cm^{-2} has the highest degree of (100) preferred orientation.

Figure 2 shows FTIR spectra of the post-implantation annealed and annealed $La_{0.7}Sr_{0.3}MnO_3$ films in the range of 400 - 1000 cm^{-1}. An optical phonon band is observed at about 600 cm^{-1}, corresponding to the Mn-O stretching vibration in the MnO_6 octahedron [14]. As can be seen, the frequency of Mn-O stretching vibration mode of the post-implantation annealed films implanted at 30 kV/5×10^{15} ions·cm^{-2}, 50 kV/5×10^{15} ions·cm^{-2} and 50 kV/5×10^{16} ions·cm^{-2} is 593.8 cm^{-1}, 583.0 cm^{-1} and 586.3 cm^{-1}, respectively. Clearly, the bond location of the post-implantation annealed films shifts towards high frequency compared with that of the annealed film.

The higher the stretching vibration frequency of Mn-O bond is, the shorter the length of Mn-O bond is. It implies that the Mn-O bond length of the post-implantation annealed films is shorter than that of the annealed film and can be adjusted by changing the implantation voltage and implantation dose. The shortening of Mn-O bond can enhance the double exchange interaction, which is propitious to the increase of metal-insulator transition temperature.

3.2. Morphologies of the Films

The AFM surface morphologies of the post-implantation annealed and annealed films are shown in **Figure 3**. By comparing the surface morphologies of these films with that of the as-grown film given in the reference [16], it can be found that there are plenty of new particles on the surfaces of the former. It indicates that the post-implantation annealed and annealed films regrow during annealing process. The new particles on the surface of the annealed film present in dispersive island bulges form. However, the new particles on the surfaces of the post-implantation annealed films are relatively uniform in size and close in arrangement and grow along the direction perpendicular to the surface of the films. Moreover, increasing implantation voltage or implantation dose can result in an obvious decrease in size of the new particles. The AFM results also show that the films have different surface roughness R_a. The R_a of the annealed film is 3.058 nm. The R_a is 7.140 nm, 2.346 nm and 3.183 nm for the post-implantation annealed film implanted at 30 kV/5×10^{15} ions·cm^{-2}, 50 kV/5×10^{15} ions·cm^{-2} and 50 kV/5×10^{16} ions·cm^{-2}, respectively. Clearly, the treatment of implanting with Al and post-implantation annealing can effectively adjust the surface morphology and surface roughness of $La_{0.7}Sr_{0.3}MnO_3$ films.

3.3. Metal-Insulator Transition of the Films

In order to understand the effect of the treatment of implanting with Al and post-implantation annealing on the transport property of the films, the temperature dependence of resistivity of the films was measured. But the
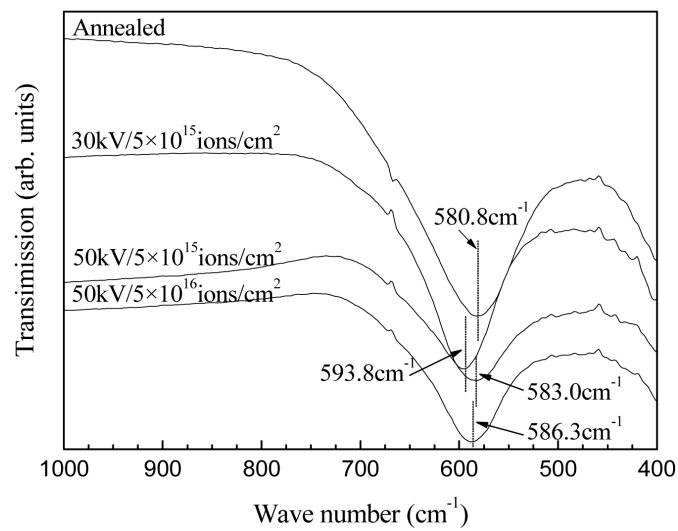
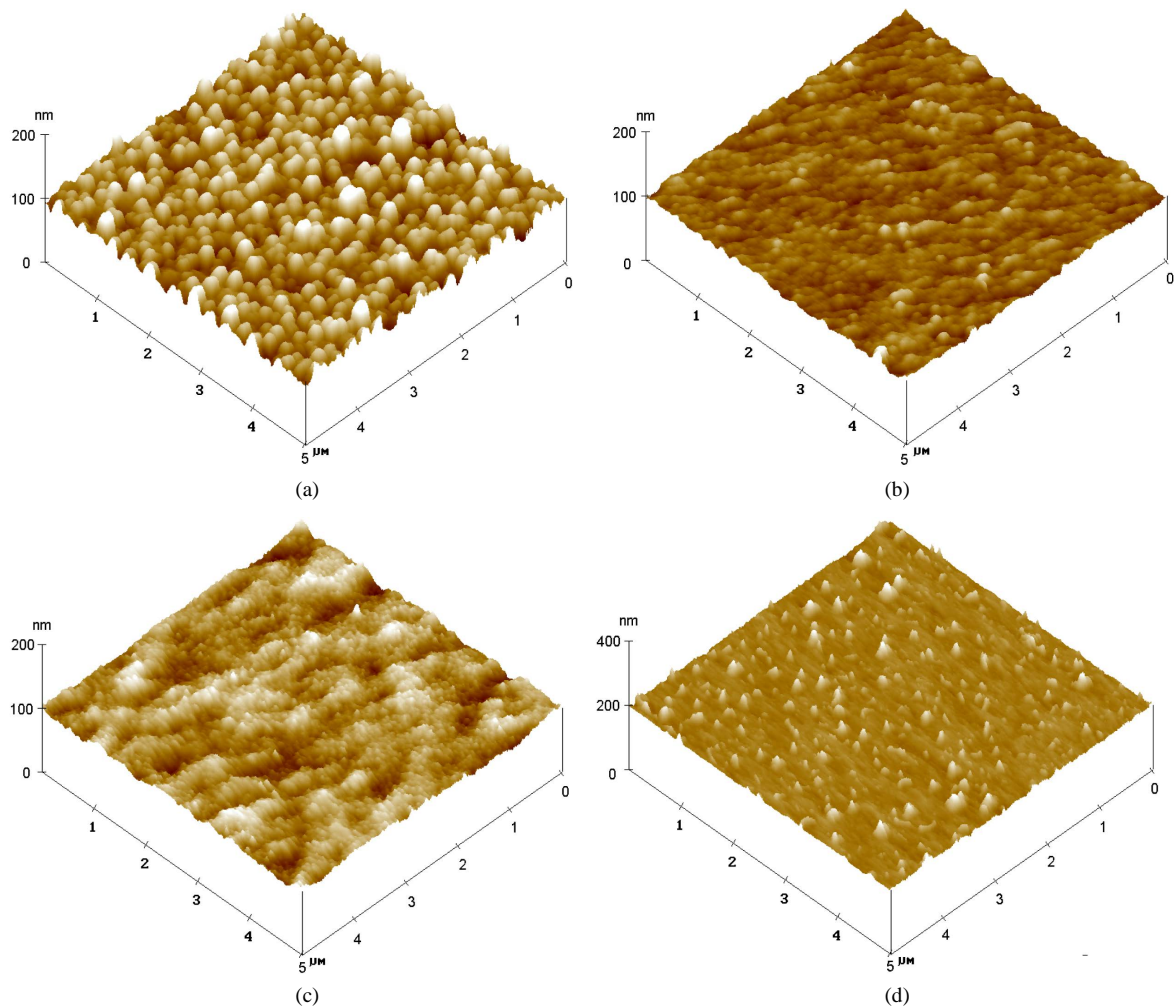**Figure 2.** FTIR of the post-implantation annealed and annealed $La_{0.7}Sr_{0.3}MnO_3$ films.

Figure 3. Surface morphologies of the $La_{0.7}Sr_{0.3}MnO_3$ films: (a) Film 2 (30 kV/5 × 10^{15} ions·cm^{-2}); (b) Film 3 (50 kV/5 × 10^{15} ions·cm^{-2}); (c) Film 4 (50 kV/5 × 10^{16} ions·cm^{-2}); (d) Film 1 (annealed).

measurement of the post-implantation annealed film implanted at 50 kV/5 × 10^{15} ions·cm^{-2} failed due to high resistance over the range of the used instrument, which indicates that this film is insulation state in the measuring temperature range. The temperature dependence of resistivity of the other three films is shown in **Figure 4**. As can be seen, the films exhibit metal-insulator transition and similar change tendency of resistivity with temperature. The T_{MI} is 221 K, 214 K and 247 K for the annealed film, post-implantation annealed film implanted at 30 kV/5 × 10^{15} ions·cm^{-2} and post-implantation annealed film implanted at 50 kV/5 × 10^{16} ions·cm^{-2}, respectively. Clearly, the T_{MI} of the post-implantation annealed films depends on implantation voltage and implantation dose, which can be higher or lower than T_{MI} of the annealed film. It is worthwhile to note that the T_{MI} and resistivity of the post-implantation film implanted at 30 kV/5 × 10^{15} ions·cm^{-2} decrease at the same time compared with those of the annealed film. Usually, the La$_{1-x}$Sr$_x$MnO$_3$ with low T_{MI} has a relative high resistivity [9] [17]. The effect of the treatment of implanting with Al and post-implantation annealing on the transport property of La$_{0.7}$Sr$_{0.3}$MnO$_3$ film can be explained as following. When the film is implanted with Al at 30 kV, a thin Al layer is deposited on the surface of the film due to relative weak implantation effect. During annealing process, the thin Al layer is easily oxidized to form discontinuous Al$_2$O$_3$. The presence of Al$_2$O$_3$ depresses in-diffusion of oxygen and then weakens the oxidation degree of the film, which can results in more oxygen vacancy defects in the film. Moreover, a part of Mn^{3+}-O^{2-}-Mn^{4+} double exchange channels become Al^{3+}-O^{2-}-Mn^{4+} because some of the implanted Al can occupy the Mn site. Therefore, the post-implantation annealed film implanted at 30 kV has a lower T_{MI} than the annealed film due to the weakening of double exchange interaction. On the other hand, the implanted Al can result in the decrease of resistivity of the film due to its excellent conductivity. When the film is implanted with Al at 50 kV/5 × 10^{16} ions·cm^{-2}, the content of Al deposited on the surface of the film decreases due to the enhancement of implantation effect. Aluminum is easy to be oxidized. The presence of the Al implanted into the film and vacancy defects induced by implanting with Al can effectively improve the oxidation uniformity and oxidation degree of the film, which can result in the improvement of microstructure of the film. It is propitious to metal-insulator transition. So the post-implantation annealed film implanted at 50 kV/5 × 10^{16} ions·cm^{-2} has a higher T_{MI} than the annealed film. This agrees with Ravi Bathe's view. They suggested that the increase of T_{MI} of the post-implantation annealed La$_{2/3}$Ca$_{1/3}$MnO$_3$ films resulted from uniformly oxygenating and the improving microstructure of the films due to the presence of Ag implanted into the films [18]. Obviously, the metal-insulator transition property of the La$_{0.7}$Sr$_{0.3}$MnO$_3$ films can be adjusted efficiently by the treatment of implanting with Al and post-implantation annealing. In our case, the T_{MI} can change from 10 – 247 K at least. Implanting with Al at low voltage or low dose will result in the decrease of T_{MI} of the post-implantation annealed La$_{0.7}$Sr$_{0.3}$MnO$_3$ films. The change of T_{MI} will obviously affect the emittance property of La$_{0.7}$Sr$_{0.3}$MnO$_3$ films.

3.4. Room Temperature Emittance of the Films

Figure 5 gives the IR reflectance spectra from 2.5 to 25 μm at room temperature of the films. It can be found that the post-implantation annealed films have a higher reflectance than the annealed film and the difference of
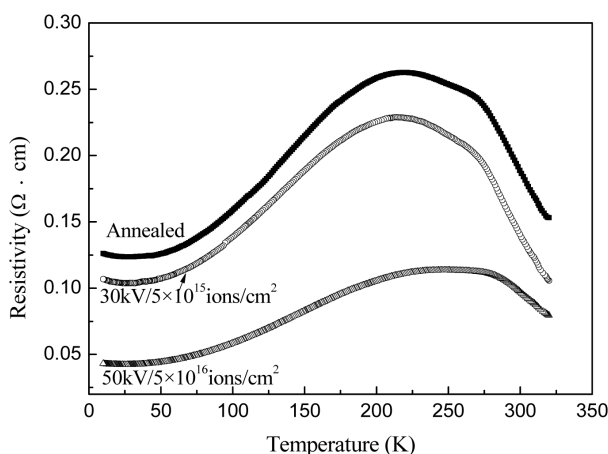

Figure 4. Temperature dependence of resistivity of the post-implantation annealed and annealed La$_{0.7}$Sr$_{0.3}$MnO$_3$ films.

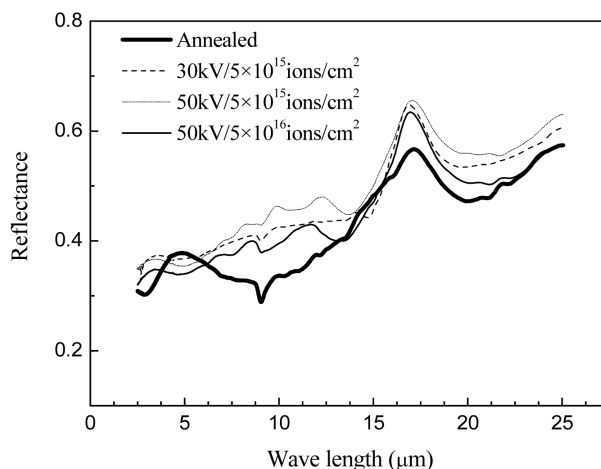**Figure 5.** IR reflectance spectra at room temperature of the post-implantation annealed and annealed $La_{0.7}Sr_{0.3}MnO_3$ films.

reflectance is small for the post-implantation annealed films. As these films are nontransparent, the emittance of them can be evaluated based on their reflectance as per the followed formula [14] where $I_b(\lambda, T)$ is blackbody spectral intensity, $R(\lambda)$ is reflectance, λ is wavelength, T is temperature and λ_i (i = 1, 2) represents the initial wavelength and end wavelength of a certain wavelength range, respectively. It should be noted that the blackbody spectral emittance from 2.5 μm to 25 μm covers nearly 85% to the total emittance. According to the formula (1), the emittance at room temperature of the post-implantation annealed films decreases slightly compared with that of the annealed film and the changes of implantation voltage and implantation dose result in a small difference in the room temperature emittance. The change of the emittance at room temperature mainly results from the combined action of surface roughness, composition and preferred orientation of the films. According to the GXRD result, it can be found that the films with (100) preferred orientation have a relative low emittance at room temperature.

$$\varepsilon = \frac{\int_{\lambda_1}^{\lambda_2} (1 - R(\lambda)) I_b(\lambda, T) d\lambda}{\int_{\lambda_1}^{\lambda_2} I_b(\lambda, T) d\lambda} \tag{1}$$

4. Conclusions

The post-implantation annealed $La_{0.7}Sr_{0.3}MnO_3$ films exhibit single perovskite phase and obvious (100) preferred orientation growth. The degree of (100) preferred orientation, Mn-O bond length, surface roughness and metal-insulator transition temperature of these films can be adjusted by changing the implantation voltage and implantation dose of Al. Compared with the annealed film, the post-implantation annealed films have shorter Mn-O bond length and lower room temperature emittance. However, the T_{MI} change tendency of the post-implantation annealed films strongly depends on the implantation voltage and implantation dose. The post-implantation annealed films implanted with Al at low voltage or low dose have lower T_{MI} than the annealed film due to the degradation of oxidation degree and the part displacement of Mn^{3+}-O^{2-}-Mn^{4+} by Al^{3+}-O^{2-}-Mn^{4+}. The post-implantation annealed film implanted with Al at 50 kV/5 × 10^{16} ions·cm^{-2} has higher T_{MI} than the annealed film because the improvement of microstructure of the film promotes metal-insulator transition. The changes of implantation voltage and implantation dose have only a small effect on the room temperature emittance of the post-implantation annealed films. By comparison, the modified $La_{0.7}Sr_{0.3}MnO_3$ films with (100) preferred orientation have relatively lower emittance at room temperature.

Acknowledgements

References

[1] Tang, G.C., Yu, Y., Chen, W. and Cao, Y.Z. (2008) Thermochromic Properties of Manganese Oxides $La_{1-x}A_xMnO_3$ (A=Ca, Ba). *Materials Letters*, **62**, 2914-2916. http://dx.doi.org/10.1016/j.matlet.2008.01.074

[2] Wu, C.H., Qiu, J.W., Wang, J.B., Xu, M. and Wang, L.X. (2010) Thermochromic Property of $La_{0.8}Sr_{0.2}MnO_3$ Thin-Film Material Sputtered on Quartz Glass. *Journal of Alloys and Compounds*, **506**, L22-L24. http://dx.doi.org/10.1016/j.jallcom.2010.07.112

[3] Shimakawa, Y., Yoshitake, T., Kubo, Y., Machida, T., Shinagawa, K., Okamoto, A., Nakamura, Y., Ochi, A., Tachikawa, S. and Ohnishi, A. (2002) A Variable-Emittance Radiator Based on a Metal-insulator Transition of (La, Sr) MnO_3 Thin Films. *Applied Physics Letters*, **80**, 4864-4866. http://dx.doi.org/10.1063/1.1489079

[4] Shen, X.M., Xu, G.Y. and Shao, C.M. (2010) Influence of Structure on Infrared Emissivity of Lanthanum Manganites. *Physica B*: *Condensed Matter*, **405**, 1090-1094. http://dx.doi.org/10.1016/j.physb.2009.11.011

[5] Tang, G.C., Yu, Y., Cao, Y.Z. and Chen, W. (2008) The Thermochromic Properties of $La_{1-x}Sr_xMnO_3$ Compounds. *Solar Energy Materials & Solar Cells*, **92**, 1298-1301. http://dx.doi.org/10.1016/j.solmat.2008.05.001

[6] Fan, D.S., Li, Q. and Xuan, Y.M. (2011) Emissivity and Optical Properties of Thermochromic Material $La_{0.7}Ca_{0.3-x}Sr_xMnO_3$ ($0 \le x \le 0.3$). *International Journal of Thermophysics*, **32**, 2127-2138. http://dx.doi.org/10.1007/s10765-011-1062-3

[7] Shimazaki, K., Tachikawa, S., Ohnishi, A. and Nagasaka, Y. (2001) Radiative and Optical Properties of $La_{1-x}Sr_xMnO_3$ ($0 \le x \le 0.4$) in the Vicinity of Metal-insulator Transition Temperatures from 173 to 413K. *International Journal of Thermophysics*, **22**, 1549-1561. http://dx.doi.org/10.1023/A:1012813625195

[8] Jiang, S.Q., Ma, X.X., Tang, G.Z., Wang, Z.H., Wang, G. and Zhou, Z.H. (2011) Microstructure and Variable Emittance Property of Annealed La-Sr-Mn-O Films. *Journal of Rare Earths*, **29**, 83-86. http://dx.doi.org/10.1016/S1002-0721(10)60407-3

[9] Urushibara, A., Moritomo, Y., Arima, T., Asamitsu, A., Kido, G. and Tokura, Y. (1995) Insulator-Metal Transition and Giant Magnetoresistance in $La_{1-x}Sr_xMnO_3$. *Physical Review B*, **51**, 14103-14109. http://dx.doi.org/10.1103/PhysRevB.51.14103

[10] Rodríguez-Martínez, L.M., Ehrenberg, H. and Attfield, J.P. (2000) Disorder Effects on Structural and Electronic Transitions in High Tolerance Factor Manganite Perovskites. *Solid State Science*, **2**, 11-16. http://dx.doi.org/10.1016/S1293-2558(00)00117-5

[11] Venkataiah, G., Prasad, V. and Reddy, P.V. (2007) Influence of A-Site Cation Mismatch on Structural, Magnetic and Electrical Properties of Lanthanum Manganites. *Journal of Alloys and Compounds*, **429**, 1-9. http://dx.doi.org/10.1016/j.jallcom.2006.03.081

[12] Tang, G.C., Yu, Y., Chen, W. and Cao, Y.Z. (2008) The Electrical Resistivity and Thermal Infrared Properties of $La_{1-x}Sr_xMnO_3$ compounds. *Journal of Alloys and Compounds*, **461**, 486-489. http://dx.doi.org/10.1016/j.jallcom.2007.07.021

[13] Jiang, S.Q., Tang, G.Z., Ma, X.X. and Yukimura, K. (2012) Emissivity of $La_{1-x}Sr_xMnO_3$/Acrylic Resin Thermal Control Coating. *Rare Metal Materials and Engineering*, **41**, 253-255.

[14] Jiang, S.Q., Ma, X.X., Wang, G., Tang, G.Z., Wang, Z.H. and Zhou, Z.H. (2013) Characteristics of $La_{0.7}Sr_{0.3}MnO_{3-\delta}$ Films Treated by Oxygen Plasma Immersion Ion Implantation. *Surface & Coatings Technology*, **229**, 76-79. http://dx.doi.org/10.1016/j.surfcoat.2012.04.013

[15] Lanke, U.D. (1999) An Attempt to Replace an Anion in CMR Oxide: Nitrogen Implantation in $La_{0.75}Ca_{0.25}MnO_3$. *Nuclear Instruments and Methods in Physics Research B*, **155**, 85-90. http://dx.doi.org/10.1016/S0168-583X(99)00238-4

[16] Jiang, S.Q., Ma, X.X., Tang, G.Z., Wang, G., Wang, Z.H. and Zhou, Z.H. (2011) Microstructure and Nano-Scratch Behaviors of $La_{0.7}Sr_{0.3}MnO_3$ Films. *Thin Solid Films*, **519**, 4880-4883. http://dx.doi.org/10.1016/j.tsf.2011.01.046

[17] Moritomo, Y., Asamitsu, A. and Tokura, Y. (1995) Pressure Effect on the Double-Exchange Ferromagnet $La_{1-x}Sr_xMnO_3$ ($0.15 \le x \le 0.5$). *Physical Review B*, **51**, 16491-16494. http://dx.doi.org/10.1103/PhysRevB.51.16491

[18] Bathe, R., Adhi, K.P., Patil, S.I., Marest, G., Hannoyer, B. and Ogale, S.B. (2000) Silver Ion Implantation in Epitaxial $La_{2/3}Ca_{1/3}MnO_3$ Thin Films: Large Temperature Coefficient of Resistance for Bolometric Applications. *Applied Physics Letters*, **76**, 2104-2106. http://dx.doi.org/10.1063/1.126269